

NO COPY RESOLUTION TEST CHART

AD-A189 558



Resonator Coupling of Two
Ring Cavity, Argon-Ion Lasers

THESIS

Warren O. Abraham
Captain, USAF

AFIT/GEO/ENP/87D-1

DTIC
ELECTE
MAR 03 1988
S D
E

DEPARTMENT OF THE AIR FORCE
AIR UNIVERSITY
AIR FORCE INSTITUTE OF TECHNOLOGY

Wright-Patterson Air Force Base, Ohio

This document has been approved
for public release and sale; its
distribution is unlimited.

88 3 01 117

AFIT/GEO/ENP/87D-1

1

Resonator Coupling of Two
Ring Cavity, Argon-Ion Lasers

THESIS

Warren O. Abraham
Captain, USAF

AFIT/GEO/ENP/87D-1

Approved for public release; distribution unlimited

SECRET
D

Resonator Coupling of Two Ring Cavity,
Argon-Ion Lasers

THESIS

Presented to the Faculty of the School of Engineering
of the Air Force Institute of Technology
Air University
In Partial Fulfillment of the
Requirements for the Degree of
Master of Science in Electrical Engineering



Warren O. Abraham
Captain, USAF

December 1987

Accession For	
NTIS GRA&I	<input checked="" type="checkbox"/>
DTIC TAB	<input type="checkbox"/>
Unannounced	<input type="checkbox"/>
Justification	
By _____	
Distribution/	
Availability Codes	
Dist	Avail and/or Special
A-1	

Approved for public release; distribution unlimited

Acknowledgements

Undertaking this thesis topic has provided me with invaluable "hands-on" experience. Although the theoretical investigation I completed was rewarding, "playing" with the hardware was even more enjoyable. Lasers and their operation have always interested me and I'm glad I had the opportunity to study them.

I would like to thank my advisor, Dr. Won B. Roh for the guidance and patience he gave me as I proceeded with this investigation. I'd also like to thank Mark Jelonek, my "advisor-behind-the-scenes", for the helpful suggestions and encouragement he provided throughout my experiment. Mark Kramer of the Air Force Weapons Laboratory at Kirtland AFB, NM, is also deserving of my gratitude. Without his advice, my results would have taken much longer to acquire. Finally, I want to thank my wife, Rebecca, for her support of and patience with me as I completed this thesis.

Table of Contents

	Page
Acknowledgements	ii
List of Figures	iv
Abstract	v
I. Introduction	1
II. Theory	8
Superposition of Two Waves	8
Spencer and Lamb's Theory.	13
III. Experimental Setup	17
Experimental Configuration	17
Ring Cavity Alignment	23
Coupling Alignment	25
IV. Results and Analysis	29
Phase I: Backward Coupling	29
Phase II: Backward and Forward Coupling	31
Phase III: Backward and Strong Forward Coupling	35
Analysis	39
Generalization 1	39
Generalization 2	40
V. Conclusions and Recommendations	44
Bibliography	47
Vita	48

List of Figures

Figure	Page
1. Superposition of Two Plane Waves.	9
2. Coupled Resonators	14
3. Schematic Diagram of Experimental Setup	18
4. Orientation of Coupling Beamsplitters	27
5. Second Orientation of Coupling Beamsplitters	28
6a. Superposition of Single and Multimode Output	33
6b. Increase Amplitude of Single Mode Signal	33
7. Photodiode Trace for Phased Output of Two Rings (One Ring Operated Single Mode/ One Multimode)	34
8. Photodiode Output for Retroreflection of the Forward Traveling-wave	37
9. Phase Locking Activity with Strong Retroreflection of the Forward Traveling-wave	38

Abstract

This thesis reports on a study of phasing two continuous-wave, resonator-coupled, argon-ion ring lasers. Rings with cavity lengths of about 3.4 meters were formed from Spectra Physics Model 164 and 165 lasers. These rings were coupled in several configurations, and portions of each ring output were combined to form a mixed beam, which was monitored for phase locking (frequency locking and coherence) with a Fabry-Perot scanning interferometer and a fast photodiode. Short term phase locking was achieved (≤ 2.5 msec) when at least one ring was operated in multimode. Precise frequency tuning of rings operating in single mode was not possible, therefore phase locking of two single mode rings was not observed. Variation of ring input current above the rings' lasing thresholds did not affect phase locking, but increasing the coupling strength between the resonators increased the duration of phase locking activity. Suppression of intracavity air turbulence increased the frequency range within which phase locking occurred.

RESONATOR COUPLING OF TWO RING CAVITY, ARGON-ION LASERS

I. INTRODUCTION

Although single laser output power has increased in recent years, the power is still not adequate for Air Force and Space Defense Initiative applications. One way to overcome this power limitation is to phase lasers. Laser phasing is the coupling of two or more lasers to produce output beams which can be coherently combined to yield peak output power which scales as the square of the number of lasers rather than the sum of the individual laser powers. By phasing several lasers, power output required for military applications can be made available.

Previous experiments have shown that phasing two or more lasers by resonator coupling can be accomplished (2,5). Most of these research efforts, however, sought only to substantiate the phasing concept, and many practical issues are still unresolved (6:3). This study investigates the resonator coupling method of laser phasing as it applies to two continuous-wave, argon-ion lasers operating in ring configuration. In addition to verifying that the output of resonator-coupled, ring-cavity lasers exhibits phase locking activity, this study characterizes effects of the following on phase locking stability of outputs from two resonator-

coupled lasers:

1. Laser mode of operation (single versus multimode).
2. Coupling configuration (forward versus backward seeding of resonators) and coupling strength.
3. Intracavity air turbulence.

Ring cavities were chosen for this investigation because they use more of the gain medium than do standing-wave cavities and, therefore, provide more laser output power. In standing-wave resonators, spatial hole burning limits the amount of gain medium used, which limits output power. Ring cavities, however, support two oppositely directed traveling-waves which may have unrelated amplitudes, phases and frequencies (4:172). Spatial hole burning is not prevalent in ring cavities, and these dissimilar traveling-waves use more of the gain medium, producing more output power.

The two traveling-waves mentioned above allow implementation of several coupling techniques. The wave traveling clockwise within the cavity is termed the forward traveling-wave, while the counter-clockwise wave is termed the backward traveling-wave. These traveling-waves produce two output beams from each ring's output coupler. The backward traveling-wave output beam leaves the output coupler at some angle other than ninety degrees, while the forward traveling-wave output beam exits perpendicular to each

output coupler. Backward traveling-wave coupling, therefore, pertains to injecting the backward traveling-wave output from one ring into the other, and vice-versa. Forward traveling-wave coupling pertains to injecting a portion of the forward traveling-wave output from one ring back into the cavity from which it originated, or into the other ring.

Resonator coupling, injection locking and master-oscillator-power-amplifier (MOPA) configuration are three prominent techniques which increase laser output power by coupling multiple components. Although the resonator coupling technique of laser phasing is similar to injection locking and MOPA coupling techniques, differences between these methods of power amplification exist. Injection locking isolates one laser in the coupled configuration from the others. This independent master oscillator affects, but is not affected by, the operation of one or more slave lasers to which it is coupled. MOPA differs from a injection-locked device in that the power amplifier in the MOPA operates below its lasing threshold. If the master oscillator's injected beam is removed, no lasing occurs from the amplifier. The slave oscillator in an injection-locked configuration, however, operates above its lasing threshold and will continue to lase after the injected beam is removed.

The resonator coupling method of laser phasing allows each laser in the coupled configuration to influence, and be

influenced by, the others. As in injection locking, all lasers in the coupled configuration operate above their lasing thresholds, therefore an injected beam is not required for individual devices to lase. The major advantage held by resonator coupling over injection locking and MOPA coupling techniques is its modularity and, consequently, its reliability. Each component in the coupled configuration is self-contained; if one component fails, the others continue to operate, providing somewhat reduced power amplification. No one component is more essential to system operation than any other. Both injection locking and MOPA coupling techniques, however, use a master oscillator which is essential to operation of the coupled system. If this oscillator fails in a MOPA system, the power amplifiers cease to lase and no output is achieved. If the master oscillator fails in an injection-locked system, individual devices continue to lase, but the outputs are not coherent, and cannot be summed. Only a resonator-coupled system continues to produce amplified laser power no matter which component fails. It is this reliability that makes resonator coupling the subject of this investigation.

Little information exists pertaining to the resonator coupling method of laser phasing. One experimental study (5), however, provides some background for the current investigation. Spencer and Lamb's theoretical description of coupled laser theory (7) provided a basis for an

experimental study completed by G. E. Palma (5). He conducted a series of experiments in which he coupled two, four, and six CO₂ lasers with unstable cavities. His study included seeding of secondary lasers with forward and backward traveling-waves from a primary master laser. He concluded that resonator coupling was easier to implement using the backward traveling-wave of the master laser, rather than using the forward traveling-wave. He also determined that use of hole coupling mirrors as resonator coupling elements was most practical for high power applications. He admitted, however, that beam splitters could be used as coupling elements for some applications (5:19). His results illustrated that "multiline, multimode, coherent outputs with a broad locking range" could be produced as a result of resonator coupling (5:18-19).

Another experimental study, conducted by S. Holswade, involved resonator coupling of two unstable CO₂ ring lasers (2). Although cavity lengths were uncontrolled and mirror mounts weren't stabilized to any great extent, mutually coherent output beams were easily obtained (2:3). These results, and those of Palma, substantiate resonator coupling as a method of laser phasing, and provide insight for this study.

Although phase locking results have been observed for resonator-coupled configurations of CO₂ lasers, phasing Argon lasers is more difficult. Frequency locking (matching laser frequencies), a requirement for phasing, is harder to

achieve using Argon than it is using CO₂ lasers. The frequency bandwidth of CO₂ lasers is about 50 megahertz, while the bandwidth of the Argon lasers used in this investigation was about 8 Ghz. Matching the frequencies of two CO₂ lasers is, therefore, much easier than matching the frequencies of two Argon lasers whose bandwidth is 160 times as great.

As an indicator of phase locking of the coupled lasers, the orientation and stability of interference fringes formed by the two output beams were used. A fast photodiode detector and oscilloscope, and polaroid camera were used to detect and document fringe formation. A scanning Fabry-Perot interferometer was used to record frequency locking of the two lasers.

Initially, resonator coupling was accomplished solely by backward traveling-wave coupling of the two ring cavities. The entire backward traveling-wave exiting the output coupler of one cavity was reflected directly into the second laser, and vice-versa. Etalons were installed in each ring cavity to suppress multimode operation, and phase locking was attempted with both lasers operating in single mode. Then, one of the etalons was removed and phase locking was investigated with one ring operating in single mode, the other in multimode. Finally, the second etalon was removed and phase locking of two rings operating in multimode was studied.

During the next portion of this investigation, coupling

was altered to include forward traveling-wave coupling of the resonators and observations for each configuration above were recorded. Then, the effects of air turbulence and forward traveling-wave coupling strength on phase locking activity were examined.

This document is organized into four chapters. Chapter II introduces theory describing the superposition of two waves, and derives an expression for the intensity at some point in an observation plane. From this expression, laser phasing is defined. Then, Spencer and Lamb's resonator coupling model is presented and their theoretical results are applied to this experiment. Chapter III describes the experimental setup and apparatus, and procedures used in this investigation. Chapters IV and V contain experimental results and analysis, and conclusions and recommendations for future research, respectively.

II. Theory

This chapter provides a theoretical basis for understanding laser phasing. First, theory describing the superposition of two plane waves is presented, an equation for intensity at a point is derived, and phasing is defined. Then, the resonator coupling method of phasing is summarized, Spencer and Lamb's coupling theory is reviewed (7), and fundamental equations describing electric fields within resonator-coupled, standing-wave cavities are introduced.

Superposition of Two Waves

Figure 1 illustrates the superposition of two waves, \vec{E}_1 and \vec{E}_2 , given by:

$$\begin{aligned}\vec{E}_1 &= \vec{E}_{01} \exp [i \cdot (\vec{k}_1 \cdot \vec{r} - \omega_1 t + \epsilon_1)] \\ \vec{E}_2 &= \vec{E}_{02} \exp [i \cdot (\vec{k}_2 \cdot \vec{r} - \omega_2 t + \epsilon_2)],\end{aligned}\tag{1}$$

where \vec{E}_{01} , and \vec{E}_{02} are the polarization vectors. Here, \vec{k}_1 and \vec{k}_2 define the direction of propagation of \vec{E}_1 and \vec{E}_2 , and have magnitudes of $\frac{2\pi}{\lambda_1}$ and $\frac{2\pi}{\lambda_2}$, respectively; ω_1

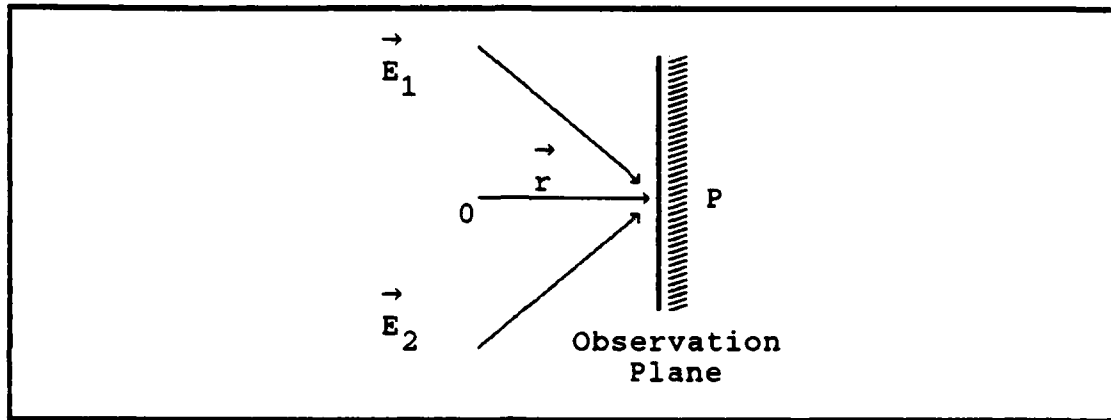


Figure 1: Superposition of Two Plane Waves.

and ω_2 are the angular frequencies, and ϵ_1 and ϵ_2 are the initial phases of \vec{E}_1 and \vec{E}_2 . The vector \vec{r} defines the position of every point in the observation plane.

To determine the intensity at some point P, the equation below must be applied:

$$I_P = |\vec{E}_{\text{total}}|^2 \quad (2)$$

Here, $\vec{E}_{\text{total}} = \vec{E}_1 + \vec{E}_2$. Therefore, the intensity at point P is given by:

$$I_P = |(\vec{E}_1 + \vec{E}_2) \cdot (\vec{E}_1 + \vec{E}_2)^*| \quad (3)$$

where \vec{E}_1^* and \vec{E}_2^* are complex conjugates of \vec{E}_1 and \vec{E}_2 .

Then

$$I_P = |E_{01}|^2 + |E_{02}|^2 + |E_{01}| |E_{02}| \cdot \cos \theta \cdot [e^{i(a-b)} + e^{i(b-a)}] \quad (4)$$

Where θ is the angle between \vec{E}_{01} and \vec{E}_{02} . Noting that $e^{ix} + e^{-ix} = 2 \cdot \cos x$, I_p can be written as:

$$I_p = |E_{01}|^2 + |E_{02}|^2 + 2 \cdot |E_{01}| |E_{02}| \cdot \cos \theta \cdot \cos [(\vec{k}_1 - \vec{k}_2) \cdot \vec{r} - (\omega_1 - \omega_2)t + \varepsilon_1 - \varepsilon_2] \quad (5)$$

If it is assumed that $|E_{01}| = |E_{02}|$, $|E_{01}|^2 = I$, and \vec{E}_{01} is parallel to \vec{E}_{02} , then I_p becomes:

$$I_p = I + I + 2 \cdot I \cdot \cos \Delta = 2 \cdot I \cdot (1 + \cos \Delta) \quad (6)$$

where $\Delta = [(\vec{k}_1 - \vec{k}_2) \cdot \vec{r} - (\omega_1 - \omega_2)t + \varepsilon_1 - \varepsilon_2]$.

Equation 6 describes the intensity at some point P located at position \vec{r} . The first term ($2I$) represents the incoherent summation of intensities from waves \vec{E}_1 and \vec{E}_2 . The second term ($2I \cdot \cos \Delta$) represents an interference term which is only present if \vec{E}_1 and \vec{E}_2 are coherent. This interference term can assume positive and negative values depending on whether the waves interfere constructively or destructively. The maximum intensity that can be achieved at point P is realized when total constructive interference occurs ($\Delta = 0$). Here, $|I_p|$ becomes $4I$. When total destructive interference occurs, $\cos \Delta \rightarrow -1$ and $|I_p| \rightarrow 0$.

To maximize the intensity due to the superposition of \vec{E}_1 and \vec{E}_2 (total constructive interference), the following conditions must be met:

$$\vec{k}_1 - \vec{k}_2 = 0, \quad \omega_1 - \omega_2 = 0, \quad \epsilon_1 - \epsilon_2 = 0.$$

It is from these conditions that phasing is defined. In order for the outputs of two lasers to constructively interfere at some point in space, $\epsilon_1 - \epsilon_2$ must be constant for all time (ie: the waves must be coherent or "in phase"). If the two laser outputs are initially in phase, but have different frequencies ($\omega_1 - \omega_2 \neq 0$), the time average of $\cos \Delta$ approaches zero and $\langle I_p \rangle \approx 2I$. Therefore, producing fixed initial phase output does not provide power amplification without frequency locking. For purposes of this thesis, then, phasing is defined as the process of both frequency locking and maintaining a fixed phase relationship between the two laser outputs.

Although the expression for I_p in equation 6 was derived for the superposition of waves from two lasers, it can easily be applied to systems of N lasers. When N lasers are phased (frequency locked and mutually coherent), the resulting intensity is scaled by N^2 (provided the intensity of each laser is I , and $\Delta = 0$). Although no energy is actually created, the summation of coherent waves alters the spatial distribution of the energy, allowing more energy (than the sum of individual intensities) to be concentrated

on axis and, subsequently, less energy (than the sum of individual intensities) to be located at other regions. By phasing lasers, a coherent summation of intensities occurs and on-axis output power is scaled above that produced by an incoherent summation of these intensities.

When beams from two unphased lasers are combined, the interference term in equation 6 fluctuates randomly, taking on both positive and negative values. The time average of these fluctuations is zero and $\langle I_p \rangle \approx 2I$. Hence, combining beams from two unphased lasers yields output intensity equal to the sum of the individual laser intensities.

When beams from two phased lasers are combined, the interference term is fixed and adds to, or subtracts from, the intensity of the superimposed beams (constructive and destructive interference). This interference produces fringes in the output intensity distribution. If Δ can be made ≈ 0 , a maximum intensity of $|I_p| = 4I$ can be achieved. Therefore, phasing lasers can increase output intensity above that produced by identical unphased lasers.

Having introduced the concept of laser phasing, it is important to understand basic theory associated with this experiment's method of phasing, resonator coupling. Of particular interest is how one characterizes coupling in analytic form. The following section briefly describes resonator coupling, derives Spencer and Lamb's description of fields within two coupled resonators, and summarizes conditions of phasing as determined by Spencer and Lamb.

Spencer and Lamb's Theory

Resonator coupling is a method of laser phasing in which each laser influences the operation of the other lasers in the coupled configuration. Feedback loops are established such that photons from each laser leak into the resonators of all other lasers. Each resonator affects, and is affected by, the other resonators to which it is coupled. Figure 2 shows the coupled-resonator configuration characterized by Spencer and Lamb (7:893). Here, the feedback loop is shown as a transmitting window which allows photons from one resonator to mix with those of the other. The boundary conditions for a standing wave cavity dictate that the resultant electromagnetic wave in resonators 1 and 2 must have a zero electric field component parallel to the surface of mirrors 1 and 2 in Figure 2 (1:201). The electric and magnetic fields in the two cavities satisfying the boundary conditions at the mirrors are:

$$\begin{aligned} E(z, t) &= \epsilon_1(t) \sin k(z + L_1), & -L_1 \leq z \leq 0 \\ E(z, t) &= \epsilon_2(t) \sin k(z - L_2), & 0 \leq z \leq L_2 \end{aligned} \quad (7)$$

where $k = \frac{2\pi}{\lambda}$ and

$$\begin{aligned} H(z, t) &= -(i/Z_0) \epsilon_1(t) \cos k(z + L_1), & -L_1 \leq z \leq 0 \\ H(z, t) &= -(i/Z_0) \epsilon_2(t) \cos k(z - L_2), & 0 \leq z \leq L_2 \end{aligned} \quad (8)$$

where $Z_0 = (\mu_0/\epsilon_0)^{1/2}$ is the impedance of free space. The electric and magnetic fields are polarized along the x and y directions, respectively, and the time dependence is described by:

$$\begin{aligned}\epsilon_1(t) &= E_1(t)e^{-i[\nu t + \phi_1(t)]}, \\ \epsilon_2(t) &= E_2(t)e^{-i[\nu t + \phi_2(t)]}.\end{aligned}\tag{9}$$

Here, $\phi_1(t)$ and $\phi_2(t)$ are the phases, and ν is the frequency of the fields.

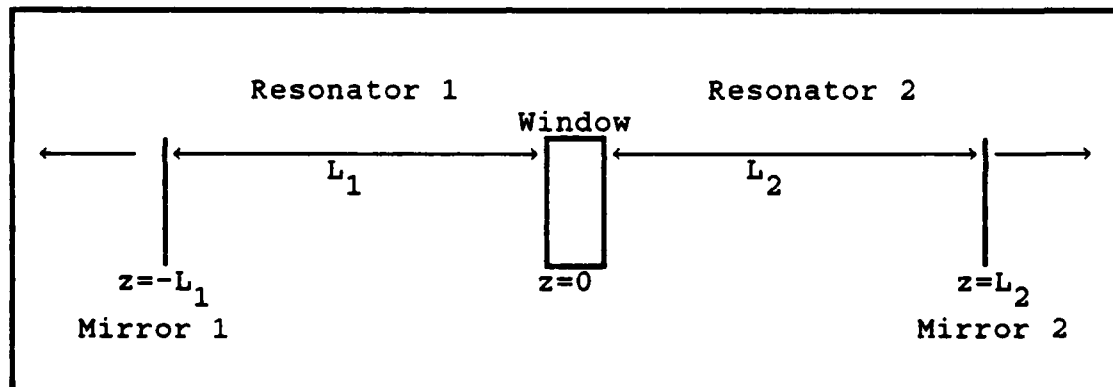


Figure 2: Coupled Resonators.

Spencer and Lamb describe the coupling window in Figure 2 as a dielectric bump located at $z=0$ with permittivity

$$\epsilon(z) = \epsilon_0 [1 + (\eta/k)\delta(z)]\tag{10}$$

where the dimensionless parameter η is related to the reflection coefficient of the window (7:893). The boundary

conditions at $z=0$ are:

$$\begin{aligned} E(0^+, t) &= E(0^-, t), \\ H(0^+, t) - H(0^-, t) &= i(\eta/Z_0)E(0, t) \end{aligned} \quad (11)$$

By assuming that the two cavities are the same length to within one wavelength, that the active media in each cavity are identical, and that the rates of excitation of the medium are the same in each cavity, Spencer and Lamb obtain four equations of motion in terms of amplitudes and phases of the electric fields given by:

$$\dot{E}_1 = [f(I_1) - \Gamma_1]E_1 + M_1E_2\sin\phi, \quad (12)$$

$$\dot{E}_2 = [f(I_2) - \Gamma_2]E_2 - M_2E_1\sin\phi, \quad (13)$$

$$\dot{\phi}_1 = \Omega_1 + M_1 - \nu + \xi f(I_1) - (M_1E_2/E_1)\cos\phi, \quad (14)$$

$$\dot{\phi}_2 = \Omega_2 + M_2 - \nu + \xi f(I_2) - (M_2E_1/E_2)\cos\phi, \quad (15)$$

where $\phi = \phi_2 - \phi_1$ is the phase difference between the fields in the two cavities, $M_j = c/(\eta L_j)$ is the coupling coefficient, $\Gamma_j = \sigma_j/\epsilon_0$ represents the cavity losses, Ω_1 and Ω_2 are the relative cavity frequencies of the coupled lasers, and $f(I_j) = [2\alpha_j/I_j \mathcal{L}(\omega - \nu)] \{1 - [1 + I_j \mathcal{L}(\omega - \nu)]^{-1/2}\}$, where $\alpha_j = (\nu \rho^2 / 2\epsilon_0 h \gamma) \bar{N}_j \mathcal{L}(\omega - \nu)$ is the gain parameter, $\mathcal{L}(\omega - \nu) = 1/(1 + \xi^2)$ is a dimensionless Lorentzian profile, $I_j = \rho^2 E_j^2 / h^2 \gamma_a \gamma_b$ is the dimensionless intensity, and the detuning of the initial frequency of the lasers ν is given by $\xi = (\omega - \nu)/\gamma$ (7:894). These equations describe the

behavior of the electric fields in standing-wave, resonator-coupled cavities.

Spencer and Lamb solved these equations for steady state using iterative techniques and observed the following results (7:894-895):

1. The only stable locked solutions occurred when the resonant frequencies of the two lasers were approximately equal.

2. When the cavity lengths of two coupled lasers were sufficiently different, the lasers operated independently.

These results verify that to phase two lasers, the operating frequencies of the coupled lasers (Ω_1 and Ω_2) must be approximately equal. The results also suggest that the cavities in this experiment should be nearly the same length to produce phased outputs.

III. Experimental Setup

This chapter first describes the experimental setup and apparatus used in this investigation. Here, specifications of optical elements and experiment parameters are given. Then, procedures used to align the ring cavities and coupling elements are summarized.

Experimental Configuration

The experimental setup is shown in Figure 3. Two commercial Spectra Physics argon-ion lasers were used, one a Model 164, the other a Model 165. Ring cavities were formed by modifying the lasers in the following manner. End mirrors and output couplers were removed from both laser housings, and the output couplers were repositioned in optical mounts using aluminum adapters. The rear end mirror of each laser was replaced by a larger flat mirror, also held in an optical mount, which was positioned approximately 20 centimeters behind each laser housing at positions A and C in Figure 3. These flat mirrors were oriented at approximately forty-five degrees with respect to the beam at positions A and C. Each new end mirror (M) reflected the intracavity beam emitted from the plasma tube off another flat turning mirror (M), oriented at about forty-eight degrees with respect to the intracavity beam at points B and D in Figure 3, to the output couplers. This ring geometry provided two output beams, one of which was used for

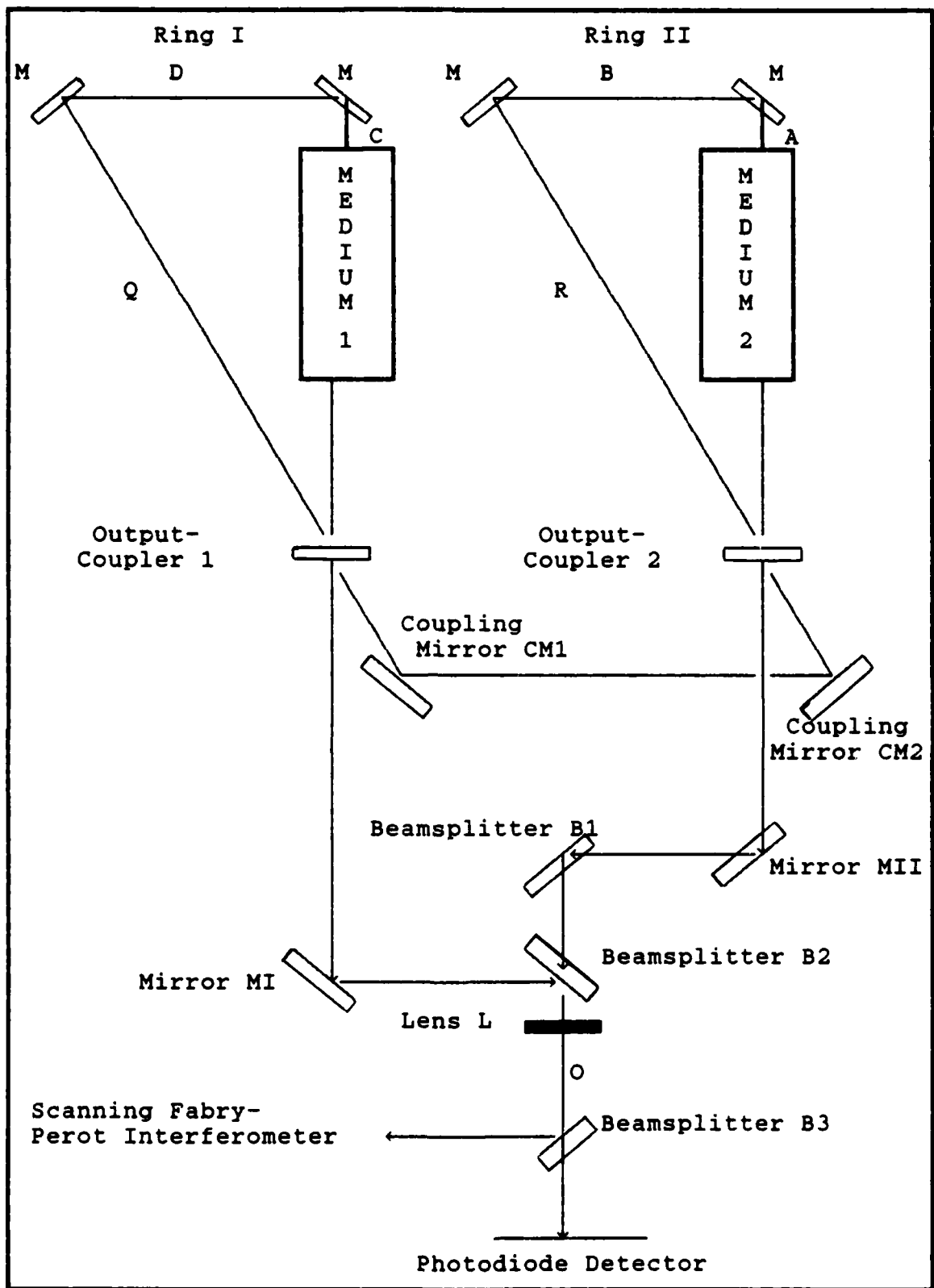


Figure 3: Schematic Diagram of Experimental Setup.

direct coupling of the backward traveling-waves from each ring (coupling beam), the other was used for diagnostics (output beam).

The mirrors (M) were flat, and were 99.8% reflective. The output couplers were spherical, 90% reflective mirrors (Output Coupler_{RingI}: radius = 4 meters; Output Coupler_{RingII}: radius = 6 meters). The cavity lengths were measured to be 3.48 meter and 3.46 meter for Ring I and Ring II, respectively.

Coupling mirrors CM1 and CM2 in Figure 3 were identical to the flat cavity mirrors above (M), and were oriented such that each coupling beam (backward traveling-wave) was fed through the rear face of the opposing ring's output coupler into its cavity, and traced the same path traveled by the ring's forward traveling-wave. The output beams from each laser were mixed as described below.

Optical elements were arranged as depicted in Figure 3 such that interference of the beams, similar to that of Young's two-slit interference, was achieved. The mixing apparatus, which consisted of wedged beamsplitters B1 and B2 (R=4 percent) located halfway between the output beams, and flat mirrors MI and MII (flat, R=100 percent), combined approximately four percent of each output beam. This configuration allowed interferometric mixture of two output beams of approximately the same intensity by maintaining nearly identical optical pathlengths and by reducing the angle at which the beams intersected to near zero. Output

from the mixing apparatus at point O in Figure 3 was then used for diagnostics.

Following beamsplitter B2, a lens L (focal length= 15 centimeters) was positioned to expand the mixed output beam. A portion of this mixed beam was directed to a scanning Fabry-Perot interferometer by beamsplitter B3 (flat, R=4 percent). The Fabry-Perot had a free spectral range of 1.5 gigahertz, and displayed the mode structure of the coupled rings on an oscilloscope. The remaining portion of the mixed beam was sampled by a photodiode detector whose output was displayed on an oscilloscope. This fast-response device detected change in intensity (which was imperceptible to the unaided eye) and displayed the intensity variation of the mixed beam on the oscilloscope. The photodiode was positioned approximately 2.5 meters from lens L in Figure 3 to allow the beam to expand, thereby reducing both the effective area of the beam sampled, and the fluctuation in beam intensity recorded on the oscilloscope. A polaroid camera was used to photograph the oscilloscope traces.

As described in Chapter II, laser phasing requires frequency locking and coherence between laser outputs. To monitor phasing a mixed beam was formed from portions of each laser output, and was sampled by the interferometer and photodiode as described above. The interferometer was used to monitor the mode structure of the coupled lasers, and indicated frequency locking, one of the conditions of phasing. The photodiode was used to monitor the intensity

variation of the mixed beam at a fixed location in the output plane of Figure 1 (fixed \vec{r}). Only when the two laser outputs were coherent would the intensity of the mixed beam vary at this location. Therefore, variation in the photodiode output indicated coherence of the lasers. Using the interferometer and the photodiode, both attributes of laser phasing could be recorded.

Throughout this experiment, the photodiode recorded intensity variation as pulses having specific width and amplitude. The width, or pulse duration, of the photodiode output is a function of phasing, and represents the period of time that both frequency locking and maintenance of a fixed phase relationship between the two laser outputs existed. The photodiode sampled a portion of the mixed output from the coupled lasers at a fixed location in the observation plane. Variation of intensity at this location was due to phasing of the laser outputs. If stable phasing occurred, one would expect the intensity at a given location to change momentarily, then remain constant as the independent laser outputs became phased. Once phased, combined output from the two lasers at a given location should not vary in intensity. The variation in intensity (pulse) recorded by the photodiode throughout this investigation resulted from unstable phasing. As $\omega_1 - \omega_2$ varied with time, fluctuations in the phased output from the lasers were detected by the photodiode (pulses). Therefore, increased pulse duration in the photodiode output

signified greater phasing stability.

The amplitude of the photodiode pulses also helped indicate phasing. The photodiode detector, which was positioned at about the center of the expanded, mixed beam output, sampled the on-axis intensity. Theory in Chapter II indicated that outputs from two phased lasers of equal intensity I would produce on-axis output intensity of $4I$. Therefore, when the lasers in this experiment were phased one would expect the on-axis intensity to change from $2I$ to $4I$, or about double. This increase in on-axis intensity, coupled with frequency locking as recorded by the Fabry-Perot interferometer, provided good indication of laser phasing.

Both cavities were aligned such that their outputs were optimized before coupling was achieved. Next, the rings were coupled such that approximately ten percent of each coupling beam was transmitted through each output coupler into the other cavity and several experimental configurations were examined.

At first, backward traveling-wave coupling was implemented, and both lasers were operated in single mode by inserting etalons in each cavity. Next, one laser's etalon was removed and phase locking was investigated with one laser operating in multimode, the other in single mode. Then, the remaining etalon was removed from its laser, and both resonators were operated in multimode.

Later, resonator interaction was increased by including

coupling of the rings' forward traveling-waves as illustrated in Figures 4 and 5 of the coupling alignment section of this chapter. Two new coupling configurations were used, and observations were documented.

A plexiglass housing protected both ring cavities from air turbulence, while the above observations were recorded. Although this housing reduced effects of laboratory air turbulence on the coupled system, perturbations still existed. Glass tubing was then installed along all intracavity and coupling beam paths. The tubing, oriented such that the laser beams were enclosed, stabilized the coupled system somewhat, and observations similar to those above were recorded.

Throughout this investigation, resonator coupling was accomplished using 488 nm light. The gain at this wavelength is higher than that at 514.5 nm (Argon's other major line), and saturates quicker. The 488 line is more nearly homogeneously broadened, and is better-suited for single-frequency operation than is Argon's 514.5 line (3:334). For these reasons, and because the ring cavities favored operation at this wavelength, Argon's 488 line was selected for use in this experiment.

Ring Cavity Alignment

Alignment of each ring cavity was accomplished as follows. The original end mirrors were initially reinstalled in the laser housings and the output couplers.

located as illustrated in Figure 3, were adjusted to optimize laser output power. These end mirrors were then removed and the new, flat end mirrors (M), located as shown in Figure 3, were oriented perpendicular to output beams at points A and C. These end mirrors, oriented to retroreflect plasma tube radiation, were adjusted to initiate lasing, and to optimize laser output power and then were rotated approximately forty-five degrees. The fluorescent spot emanating from the plasma tube was reflected off these end mirrors onto flat turning mirrors (M) as shown in Figure 3. These turning mirrors were oriented so the fluorescent reflections off their surfaces were colligned with the fluorescent spots on the end mirrors, and were then adjusted until lasing occurred, and output power was optimized.

Finally, these turning mirrors were rotated to reflect the fluorescent spot from the plasma tube off their surfaces onto the output couplers. The spots reflected by the turning mirrors were circular, purple in color, and, due to the good alignment of the output coupler, had bright white dots at their centers, as observed at points Q and R in Figure 3.

The white dots of these reflections were positioned at the center of the output couplers. Next, the output couplers were rotated to produce two reflections which could be seen on the front face of the laser housing, one due to direct reflection of the plasma tube fluorescence, the other due to fluorescent reflection from the end and turning

mirrors. By rocking the output couplers in both axes, these reflections simultaneously scanned the plasma tube and the turning mirrors. When lasing was achieved, all mirrors and output couplers were adjusted to optimize ring output power. This stepwise procedure fixed each ring's horizontal axis with regard to end and turning mirrors (M), and the plasma tube, which limited the number of variables contributing to misalignment of the ring.

Coupling Alignment

In this experiment resonator coupling was implemented in two ways. The first method coupled only the backward traveling-waves of both ring cavities. No forward traveling-wave coupling was implemented. Later, weak coupling of the forward traveling-waves was added to the backward traveling-wave coupling to stabilize phase locking. The following paragraphs outline alignment of coupling mirrors CM1 and CM2, which coupled the backward traveling-waves, and coupling beamsplitters CB1 and CB2, which coupled the forward traveling waves.

Coupling mirrors CM1 and CM2 were positioned to reflect both the coupling beam from Ring I off CM1 to CM2, and the coupling beam from Ring II off CM2 to CM1. Coupling mirror CM2 was then aligned to make Ring II's coupling beam coincident with the spot on CM1 due to Ring I's coupling beam. Once this was accomplished, coupling mirror CM1 was adjusted so Ring I's coupling beam reflected off CM1 and was

coincident with the spot on CM2 due to Ring II's coupling beam. This procedure established rough alignment of coupling mirrors CM1 and CM2.

To finely adjust the coupling alignment, Ring I's intracavity beam was blocked alternately at points C and D in Figure 3. Coupling mirror CM1 was adjusted to form unobstructed spots from Ring II's coupling beam, which were coincident with positions of Ring I's intracavity beam, on intracavity mirrors (M) of Ring I. This having been accomplished, Ring II was blocked at points A and B in Figure 3 to verify similar observations at its intracavity mirrors. When both rings exhibited the above behavior, alignment of the backward traveling-wave was considered complete.

Figure 4 shows the position and orientation of the coupling beamsplitters CB1 and CB2 used to couple the forward traveling-waves of the two rings. Initially, CB1 and CB2 were both flat, four percent reflective beamsplitters. Later, these elements were replaced with flat, 32% beamsplitters.

Alignment of beamsplitters CB1 and CB2 was difficult because each output beam was retroreflected back into its own cavity. Good alignment required the retroreflected beam to retrace the same path as each ring's intracavity beam. Since the intracavity beam and retroreflected beam were everywhere coincident, blockage of the intracavity beam to check the coupling alignment of the forward traveling-wave

also blocked the retroreflected beam. Hence, another technique for alignment was required.

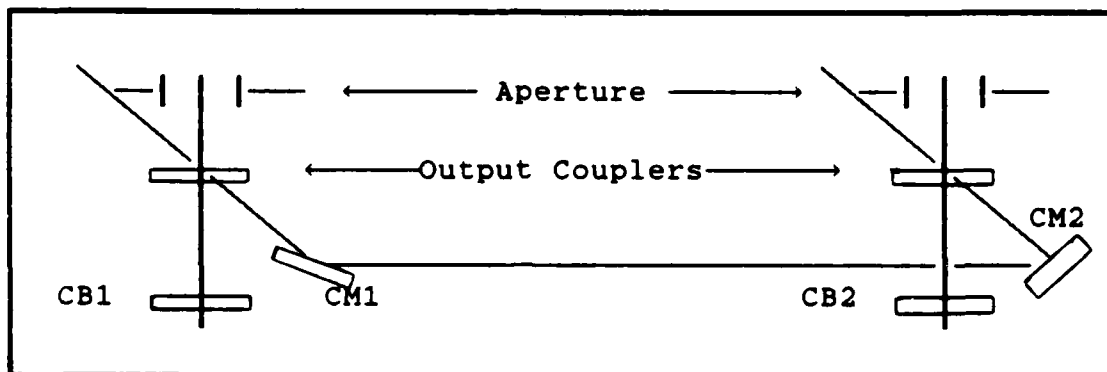


Figure 4: Orientation of Coupling Beamsplitters.

Coupling beamsplitters CB1 and CB2 were roughly aligned such that the retroreflected beams appeared to be collinear with the forward traveling-waves emitted from the output couplers. Then, an adjustable aperture was placed within each ring's cavity as shown in Figure 4 and the intracavity beam was clamped until lasing threshold was just attained. The retroreflected beam, which could be seen on the closed portion of the aperture, could then be positioned to pass through the aperture. This accomplished rough alignment of the coupling beamsplitters.

To finely adjust the alignment of these coupling beamsplitters, the mode structure of each ring was observed on the Fabry-Perot interferometer. Each ring was operated in multimode and coupling beamsplitters CB1 and CB2 were adjusted until the multimode pattern seen on the

oscilloscope gained structure. That is, the random, multimode "grasslike" output took on a more stable appearance due to the formation of a Fabry-Perot etalon between the beamsplitters and the output coupler. When both beamsplitters were thus aligned, forward traveling-wave alignment was considered complete.

One other configuration was implemented to allow controlled decoupling of the forward traveling-wave. Coupling beamsplitters CB1 and CB2 were oriented at about forty-five degrees with respect to the output beams of each ring as shown in Figure 5.

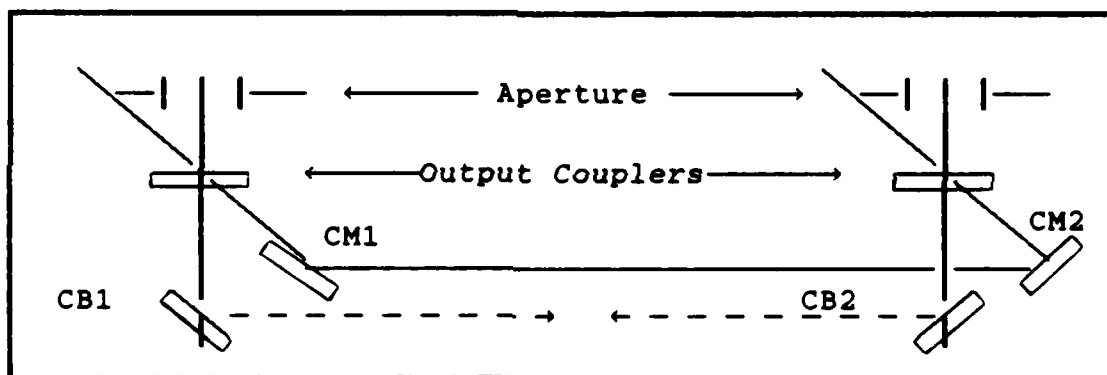


Figure 5: Second Orientation of Coupling Beamsplitters.

These beamsplitters were aligned in the same manner described above for coupling mirrors CM1 and CM2. By blocking the beam between beamsplitters CB1 and CB2, coupling of the forward traveling-waves could be interrupted, and effects on phasing could be assessed.

IV. Results and Analysis

Data collection for this investigation proceeded in three phases. During Phase I, only the backward traveling-waves of Rings I and II described in Chapter III were injected. In Phase II, however, the forward and backward traveling-waves of the ring cavities were injected into each other's cavity. This coupling configuration allowed selective decoupling of the forward traveling-waves, and provided data on the effect of forward traveling-wave coupling on phase locking stability. Finally, in Phase III both traveling-waves of Rings I and II were again coupled, but the forward traveling-wave coupling configuration was altered. Also, the coupling strength of the forward traveling-wave was increased, and intracavity air turbulence was reduced to assess the effects of these variables on phase locking stability. This chapter presents the data collected in each of these phases, and then analyzes it.

Phase I: Backward Coupling

During Phase I of this experiment, no phase locking of output beams from the two rings was observed. When one or both rings were operated in single mode, no extraordinary activity appeared in either the mode structure of the coupled configuration as displayed by the Fabry-Perot interferometer, or in the intensity variation information provided by the photodiode detector. As mentioned in

Chapter III, approximately ninety percent of each coupling beam from Rings I and II was reflected off the output couplers, and appeared in the output beam. Since the coherence length of a ring containing an etalon and operating in single mode was on the order of one meter, which was larger than the difference in optical paths traveled by a coupling beam and its reflection off the opposing ring's output coupler (about .5 meter), interference fringes were formed by interferometric mixing of these coherent beams. These intensity variations were detected by the photodiode, but were easily distinguished from phase locking activity because the magnitude of the signal was far below that expected for constructive interference of phase-locked outputs from the two ring cavities.

When both rings were operated in multimode, no phase locking intensity variation was detected by the photodiode, but unusual mode symmetry was displayed by the Fabry-Perot interferometer. The mode structure of the superposition of two, multimode ring cavities sporadically changed in the following manner. The height of several modes on both sides of the oscilloscope approximately doubled and these larger-amplitude modes traveled toward the center of the scope from each side, converged, reversed direction, and disappeared off the scope. This happened regularly and resembled a "contraction and expansion" or "breathing". This behavior was actually an illustration of short-

duration, multimode phase locking which probably resulted as modes from one ring scanned across those of the other. At certain times, the frequencies of these overlapping modes matched, and phase locking activity occurred. When the modes shifted, and frequencies became mismatched, locking activity stopped.

Input currents to both rings were varied independently between eleven and thirty-two Amps. Next, both rings were powered by equal currents, the magnitude of which was varied between eleven and thirty-two Amps. The magnitude of the currents appeared to have no effect on phase locking of the coupled configuration and no further observations were made. It was noted, however, that although the laser cavities were enclosed, intracavity air turbulence was apparent. Dust particles in the air, passing through the intracavity beam, were agitated, especially near the back of the active medium housings (near the plasma tube cooling hoses). This air turbulence might have caused or increased instability in the operating frequencies of the rings and, therefore, instability in phase locking activity. Mechanical vibrations resulting from cooling water circulating over the plasma tube, however, probably induced more instability to the system than did air turbulence.

Phase II: Backward and Forward Coupling

In Phase II of this experiment, both forward and

backward traveling-waves of Rings I and II were coupled. The coupling beamsplitters CB1 and CB2, described in Chapter III, were oriented as shown in Figure 5. Phase locking of the ring cavity output beams was observed for single mode/multimode and multimode/multimode operation of Rings I and II, while no phase locking was apparent for single mode/single mode operation. This might have resulted because the large bandwidths of the lasers and low resolution of the Fabry-Perot interferometer made it difficult to overlap the modes and match the frequencies of the two rings, which is a prerequisite for phase locking.

When one or both rings were operated in multimode, changes in both the mode structure of the coupled configuration and the intensity variation detected by the photodiode were observed. Mode structure of the unlocked output from Rings I and II operating in single mode/multimode configuration, as displayed by the Fabry-Perot interferometer, is shown in Figure 6a. Here, the superposition of single mode and multimode output can be seen. Occasionally, this mode structure changed and the single mode signal was observed to increase in amplitude as shown in Figure 6b. When this occurred, strong fluctuations were recorded by the photodiode detector. Figure 7 shows typical intensity variations recorded at instances where the

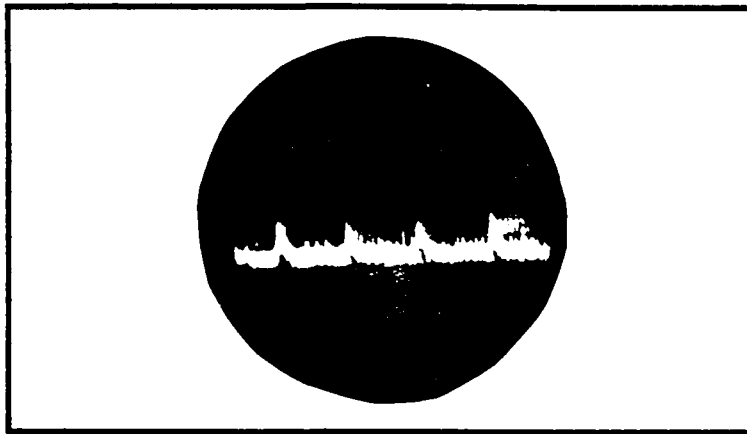


Figure 6a: Superposition of Single and Multimode Output.

mode structure of the coupled configuration appeared as in Figure 6b. This phase locking activity produced intensity

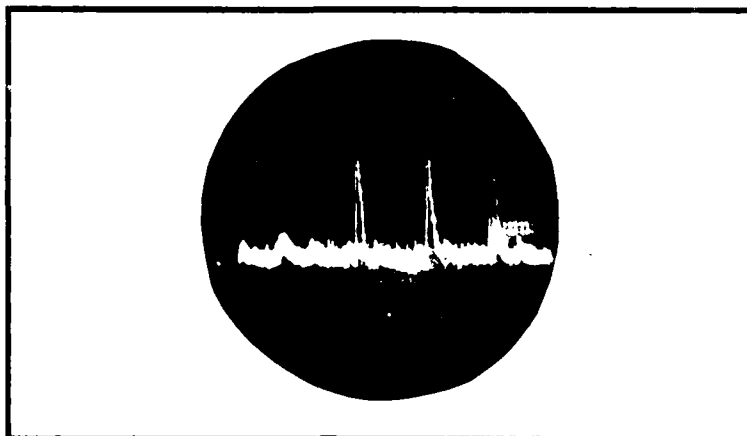


Figure 6b: Increased Amplitude of Single Mode Signal.

peaks of approximately twice the d.c. amplitude. Phase locking was random and locking duration varied between fifty and 700 microseconds.

While phase locking occurred, the backward traveling-wave coupling beam was intercepted between coupling mirrors CM1 and CM2 (see Figure 5) with an index card. Decoupling

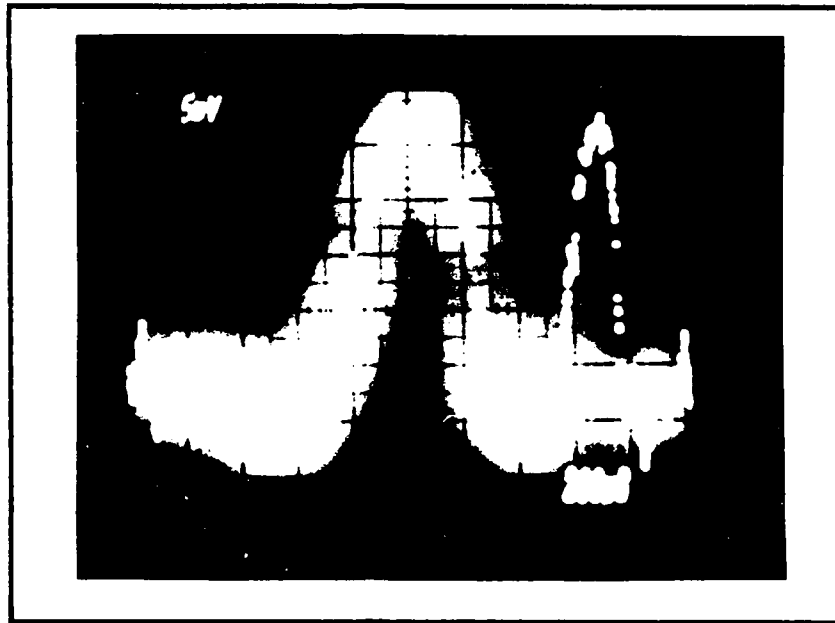


Figure 7: Photodiode Trace For Phased Output of Two Rings
(One Ring Operated Single Mode, One Multimode)

of the backward traveling-wave in this manner immediately terminated phase locking behavior of the coupled rings. Next, forward traveling-wave coupling was interrupted (by blocking the coupling beam located between coupling beamsplitters CB1 and CB2) while phase locking activity occurred. Disruption of this coupling beam had no apparent effect on phase locking of the coupled configuration. The rings continued to exhibit phase locking activity, unaltered in amplitude or duration.

When Rings I and II were both operated in multimode, phase locking was observed, but the duration of locking was shorter than that observed for single mode/multimode operation of Rings I and II. The mode structure displayed by the Fabry-Perot interferometer revealed phase locking

activity as modes from one ring swept over modes of the other. The amplitude of the intensity variation recorded by the photodiode detector was the same as that observed for single mode/multimode operation of Rings I and II, but the pulse durations were on the order of twenty microseconds.

When both rings were operated in single mode, no phase locking activity was observed. Etalons were adjusted such that mode structure from both rings was nearly coincident. Over time, the mode structure of one ring would drift across the other and the combined mode structure would grow slightly in amplitude, but no noticeable intensity variation was observed in the output during these instances. The growth of the combined mode structure was not significant compared to that shown in Figure 6b.

Input currents to both rings were varied independently, and simultaneously in the range of eleven to thirty-two amps as described in Phase I. Variation of input current appeared to have no effect on phase locking stability; only the amplitudes of the mode structure and intensity variation, as detected by the photodiode, increased. Phase locking duration and frequency of appearance remained unaltered.

Phase III: Backward and Strong Forward Coupling

During the final phase of this experiment, the forward traveling-wave coupling technique was altered. The coupling

beamsplitters CB1 and CB2 were rotated forty-five degrees such that they were perpendicular to the output beams from each output coupler. Rather than coupling one ring's forward traveling-wave to the other ring, this coupling configuration retroreflected a portion of each ring's output back into the same cavity.

This coupling configuration produced phase locking, but did not allow controlled decoupling of the forward traveling waves. As in Phase II, phase locking was observed for single mode/multimode and multimode/multimode operation of Rings I and II, but single mode operation of both rings produced no evidence of phase locking. Figure 8 shows typical intensity variations for phase-locked outputs as detected by the photodiode. Again, the amplitudes of the intensity variations are approximately twice the d.c. level, but in this coupling configuration, the duration of locking increased, and was often observed to be in the range of .75 to 1.5 milliseconds.

Next, the 4% reflective coupling beamsplitters CB1 and CB2 were replaced by 32% beamsplitters. Figure 9 shows a typical phase-locked intensity variation with these new coupling beamsplitters in place. Although phase locking

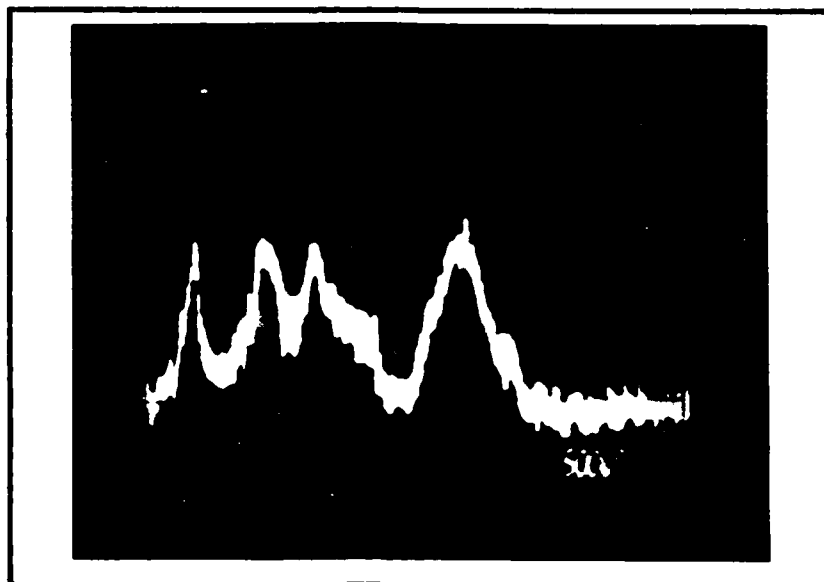


Figure 8: Photodiode Output for Retroreflection of the Forward Traveling-wave.

did not appear to be any more stable, the duration of locking increased and was observed to last up to two milliseconds.

Observations made in Phase I and Phase II with regard to intracavity air turbulence of the coupled rings prompted installation of glass tubing around intracavity and coupling beams. Approximately ninety-five percent of the paths traveled by all beams in the coupled configuration, excluding the output beams emitted or reflected by the output couplers, were enclosed by glass tubing. This stabilized intracavity air turbulence significantly, and dust was observed to remain nearly motionless inside the tubing.

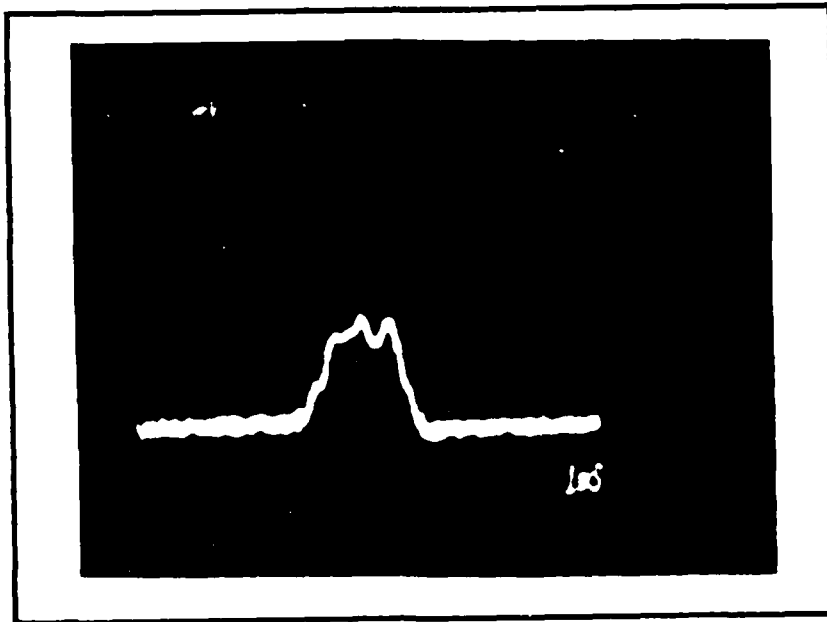


Figure 9: Phase Locking Activity with Strong Retroreflection of the Forward Traveling-wave.

The duration of phase locking did not increase as a result of atmospheric stabilization of the ring cavities, but the frequency with which phase locking activity started did. Previously, phase locking behavior would begin, last for up to thirty seconds, then stop. Dormant periods where no phase locking activity was observed often lasted five to eight minutes. After installation of glass tubing around intracavity and coupling beams, phasing activity would continue for 10 to 30 minutes, and dormant periods were shortened to tens of seconds.

As in Phase I and II, ring input currents were varied, but did not appear to affect the quality of phase locking. Phase locking was again only observed when one or neither of

the rings operated in single mode. Single mode operation of both rings produced no phase locking.

Analysis

Reviewing the experimental results presented, two generalizations about resonator coupling of ring cavities can be made. The paragraphs that follow introduce these generalizations and attempt to justify them. Afterwards, several observations are listed to summarize the remaining experimental results.

Generalization 1: It is difficult to phase two, singlemode ring lasers.

It appears that phase locking of two ring cavities operating in single mode is more difficult to achieve than is locking rings operating in single mode/multimode or multimode/multimode configuration. While no phase locking activity was observed for single mode operation of Rings I and II in coupled configuration, phase locking activity was apparent for coupled rings operating in multimode. The most vigorous phase locking activity, however, occurred for single mode/multimode operation of the two rings. These results can be explained as follows.

When both rings operated in single mode, the frequencies ω_1 and ω_2 of each ring had to be very close to achieve phase locking. Although the etalons were tuned such that the modes of one ring scanned those of the other, the

free spectral range of the Fabry-Perot interferometer was 1.5 gigahertz, so although the Fabry-Perot spectra overlapped, exact tuning of frequencies was difficult to achieve. The frequency locking range of this experimental configuration was not known, but it appeared to be quite small and tuning the ring cavities' frequencies to within this range was not possible with the instrumentation available. Since the precise mode frequencies of both cavities were not the same, phasing could not occur.

When the rings were operated in single mode/multimode configuration, more lasing frequencies of the multimode ring were available to match with the single mode, single frequency output of the other ring. When both rings were operated in multimode, frequency tuning was again possible. As the multimode structure of one ring passed over that of the other, some frequencies matched and phase locking activity occurred. This activity, however, was far more shortlived than that of rings operating in single mode/multimode configuration.

Generalization 2: Forward traveling-wave coupling is required to initiate, but not to sustain, phase locking activity.

The intent of resonator coupling is to allow photons from one resonator to interact with those of another. When backward traveling-wave coupling is implemented as in Phase

II, a portion of the backward traveling-wave of one ring is fed into the forward traveling-wave of the other ring, and vice versa. This injected radiation remains a part of the forward traveling-wave of each ring until it leaks through the output coupler, and is lost by the coupled configuration forever. These photons never return to the parent ring's backward traveling-wave. By also coupling the rings' forward traveling-waves, some of this injected radiation is fed back into the backward traveling-wave of the coupled configuration. While backward traveling-wave coupling alone does not seem to provide the rings with enough information for phase locking, "double-coupling" allows adequate interaction between rings and produces phase locking activity.

Coupling of the forward traveling-wave by retroreflection, as investigated in Phase III, also resulted in phasing activity. The coupling beamsplitters CB1 and CB2 fed photons from the forward traveling-wave of each ring into the backward traveling-wave of the same ring. Since the backward traveling-waves of both rings were coupled, "double-coupling" established a path by which photons from one ring could travel to the other and return again. As in the forward traveling-wave coupling technique discussed above, this technique provided each ring with adequate information for phase locking activity to occur.

Once established, forward traveling-wave coupling was not required to continue phase locking activity. It appears

that once the frequencies of the two rings were sufficiently close, and phase locking activity was observed, the rings were effectively locked and the cavities no longer needed the feedback provided by coupling of the forward traveling-wave. The short duration of the locking activity, however, a manifestation of frequency instability, precluded further investigation of this observation.

The following list of observations summarizes the remaining results obtained:

1. Comparing the two forward traveling-wave coupling techniques, although the configuration used during Phase II allowed controlled decoupling of the traveling-wave, the configuration used in Phase III resulted in increased duration of phase locking activity. The coupling technique used in Phase II fed the forward traveling-wave from one ring into the backward traveling-wave of the other, while Phase III's technique fed the forward traveling-wave of one ring into the backward traveling-wave of the same ring. Perhaps this difference accounts for the dissimilar behavior of the two coupling techniques.

2. Variation of the input current between eleven and thirty-two amps had no apparent effect on phase locking activity. It seems that at eleven amps input current, the coupling strengths are above the threshold needed to produce phase locking activity. However, at eleven amps input current, both rings operated well above lasing threshold, and predictions as to phase locking behavior of rings operated near lasing threshold (at input currents less than eleven amps) could not be made.

3. Increasing forward traveling-wave coupling strength increases the duration of phase locking activity. As coupling strength increases, so does interaction between the rings. With strong coupling, the rings provide each other with enough information to produce coherent outputs. With weaker coupling, ring interaction and the duration of phase locking activity decrease.

4. Suppressing intracavity and coupling beam air turbulence increased the frequency with which phase locking activity started. Intracavity air turbulence probably

influenced the operating frequency of each ring. By suppressing this turbulence, the frequencies of both rings became more stable and tuning (frequency matching) of the rings became more frequent.

V. Conclusions and Recommendations

The following paragraphs summarize conclusions from results of this investigation. First, a relationship between mode of operation for the lasers and the frequency dependence of phase locking is presented. Next, the effects of forward traveling-wave coupling and intracavity air turbulence on phasing are reviewed. Finally, recommendations for future study are offered.

Phase locking of two resonator-coupled, ring cavity, argon-ion lasers, although possible, is unstable due to fluctuations of the rings' operating frequencies. Phase locking activity was observed to last for up to 2.5 milliseconds when one ring was operated single mode and one ring in multimode because this configuration allowed cavity modes to overlap, and cavity frequencies to match. For other ring mode configurations, either frequencies could not be matched (when both rings were operated in single mode), or many frequencies matched and not enough gain was available to produce measurable phase locking activity for one particular frequency (when both rings were operated in multimode), and phase locking activity was not observed.

Forward traveling-wave coupling configurations, along with coupling strength, affect phase locking activity. Initially, both rings' forward and backward traveling-waves must be coupled to produce phase locking activity. Once established, phase locking activity persists, even when the

rings' forward traveling-waves are decoupled. Coupling of the forward traveling-waves by retroreflection (coupling forward and backward traveling-waves of the same ring) produces longer duration phase locking activity than does coupling the forward traveling-wave of each ring to the other (ie: coupling the forward traveling-wave of one ring to the backward traveling-wave of the other). Finally, by increasing the forward traveling-wave coupling strength, the duration of phase locking activity can be increased.

The importance of frequency tuning the rings to about the same frequency has been recognized as a condition for phase locking. As stated above, fluctuations in the rings' operating frequencies cause phase locking instability. By enclosing the lasers with a plexiglass housing, and the intracavity beams with glass tubing, intracavity air turbulence was suppressed, frequency fluctuations were damped, and the frequency with which phase locking activity occurred increased.

Based upon results of this investigation, several recommendations for future study can be made. First, the coupling strength of the forward and backward traveling-waves could be varied and the optimum coupling strength of both traveling waves could be determined. Another recommendation is to increase the resolution (decrease the free spectral range) of the spectrum analyzer used to monitor the coupled rings' mode structure. This would allow more exact tuning of single mode output than

could be achieved in this study, which might produce phase locking activity when both rings operate in single mode. Then, to study effects of variation of input current on phase locking activity near threshold, one ring could be spoiled (does not operate above its lasing threshold at low input current) by adding loss to the cavity. This could verify what effect input current has on phase locking.

Next the use of nonlinear optics in the coupling configuration could be investigated. These optics should compensate for cavity pathlength differences and may relax frequency locking constraints (broaden the frequency-locking range) required for phasing. Finally, perhaps resonator coupling of standing-wave cavities should be investigated. Standing-wave resonators require only one coupling path, as opposed to two for traveling-wave resonators, and should be easier to couple.

Bibliography

1. Hecht, Eugene and Alfred Zajac. Optics. Massachussets: Addison-Wesley Publishing Company, 1979.
2. Holswade, Lt S. et al. "Phase Locking of Ring Lasers." Unpublished report. Air Force Weapons Laboratory, Kirtland AFB NM (1987).
3. Man, C. N. and A. Brillet. "Injection Locking of Argon-ion Lasers," Optics Letters, 9: 333-334 (August 1984).
4. Murray, Sargent III et al. Laser Physics. Massachussets: Addison-Wesley Publishing Company, 1974.
5. Palma, G. E. et al. Coupled Resonator Beam Combining Investigation. Air Force Weapons Laboratory, AFWL-TR-85-94 Kirtland AFB, New Mexico, April 1985.
6. Roh, Won B., Application of Nonlinear Optical Techniques to Coupling and Phasing of Multiple Laser Devices and Other Optical Systems. Research Proposal submitted to Air Force Office of Scientific Research. Air Force Institute of Technology (AU), Wright-Patterson AFB, OH, 26 January 1987.
7. Spencer, Martin B. and Willis E. Lamb. "Theory of Two Coupled Lasers." Physical Review, 5:893-898 (February 1972).

Vita

Captain Warren O. Abraham was born on 8 December 1959 in Dover, New Jersey. He graduated from Roxbury High School in Succasunna, New Jersey in 1978. He attended Rutgers University where he received a Bachelor of Science in Electrical Engineering in 1982. Upon graduation he attended Officer Training School at Lackland AFB, Texas where he received a commission in the USAF, and was immediately called to active duty in September 1982. He served as Chief, Spacecraft Operations Team at Sunnyvale AFS, Sunnyvale, California until October 1983. He was then stationed at Eglin AFB, Florida, where he served as Test Engineer for the 3246 Test Wing. He was reassigned to the Hardened Target Weapons SPO, Armament Division, in May 1985 where he served until entering the School of Engineering, Air Force Institute of Technology, in June 1986.

REPORT DOCUMENTATION PAGE

Form Approved
OMB No. 0704-0188

1. REPORT SECURITY CLASSIFICATION UNCLASSIFIED		1b. RESTRICTIVE MARKINGS N/A	
2a. SECURITY CLASSIFICATION AUTHORITY		3. DISTRIBUTION/AVAILABILITY OF REPORT Approved for public release; distribution unlimited.	
2b. DECLASSIFICATION/DOWNGRADING SCHEDULE		5. MONITORING ORGANIZATION REPORT NUMBER(S)	
4. PERFORMING ORGANIZATION REPORT NUMBER(S) AFIT/GEO/ENP/87D-1		7a. NAME OF MONITORING ORGANIZATION	
6a. NAME OF PERFORMING ORGANIZATION School of Engineering	6b. OFFICE SYMBOL (if applicable) AFIT/ENG	7b. ADDRESS (City, State, and ZIP Code)	
6c. ADDRESS (City, State, and ZIP Code) Air Force Institute of Technology (AU) Wright-Patterson AFB, Ohio, 45433-6583		9. PROCUREMENT INSTRUMENT IDENTIFICATION NUMBER	
8a. NAME OF FUNDING/SPONSORING ORGANIZATION	8b. OFFICE SYMBOL (if applicable)	10. SOURCE OF FUNDING NUMBERS	
8c. ADDRESS (City, State, and ZIP Code)		PROGRAM ELEMENT NO.	PROJECT NO.
		TASK NO.	WORK UNIT ACCESSION NO.
11. TITLE (Include Security Classification) RESONATOR COUPLING OF TWO RING CAVITY, ARGON-ION LASERS.			
12. PERSONAL AUTHOR(S) Warren O. Abraham, Capt, USAF			
13a. TYPE OF REPORT MS Thesis	13b. TIME COVERED FROM _____ TO _____	14. DATE OF REPORT (Year, Month, Day) 87-12	15. PAGE COUNT 55
16. SUPPLEMENTARY NOTATION			
17. COSATI CODES		18. SUBJECT TERMS (Continue on reverse if necessary and identify by block number)	
FIELD	GROUP	Lasers, Phase Locking, Frequency Locking, Ring Lasers, Argon-Ion Lasers	
09	03		
19. ABSTRACT (Continue on reverse if necessary and identify by block number) Won B. Roh			
20. DISTRIBUTION/AVAILABILITY OF ABSTRACT <input checked="" type="checkbox"/> UNCLASSIFIED/UNLIMITED <input type="checkbox"/> SAME AS RPT <input type="checkbox"/> DTIC USERS		21. ABSTRACT SECURITY CLASSIFICATION UNCLASSIFIED	
22a. NAME OF RESPONSIBLE INDIVIDUAL Won B. Roh, Professor of Engineering Physies		22b. TELEPHONE (Include Area Code) 513-255-4498	22c. OFFICE SYMBOL AFIT/ENP

Approved for public release; distribution is unlimited.
 Approved for Release and Technical Development
 Air Force Research and Development
 Wright-Patterson AFB, OH 45433

Warren O. Abraham 31 Dec 87

This thesis reports on a study of phasing two continuous-wave, resonator-coupled, argon-ion ring lasers. Rings with cavity lengths of about 3.4 meters were formed from Spectra Physics Model 164 and 165 lasers. These rings were coupled in several configurations, and portions of each ring output were combined to form a mixed beam, which was monitored for phase locking (frequency locking and coherence) with a Fabry-Perot scanning interferometer and a fast photodiode. Short term phase locking was achieved (2.5 msec) when at least one ring was operated in multimode. Precise frequency tuning of rings operating in single mode was not possible, therefore phase locking of two single mode rings was not observed. Variation of ring input current above the rings' lasing thresholds did not affect phase locking, but increasing the coupling strength between the resonators increased the duration of phase locking activity. Suppression of intracavity air turbulence increased the frequency range within which phase locking occurred.

END

DATE

3-88

DTIC